HHS Public Access

Author manuscript

J Tissue Eng Regen Med. Author manuscript; available in PMC 2019 January 01.

Published in final edited form as:

J Tissue Eng Regen Med. 2018 January ; 12(1): 191–203. doi:10.1002/term.2395.

Angiogenic and osteogenic regeneration in rats via calcium phosphate scaffold and endothelial cell coculture with hBMSCs, hUCMSCs, hiPSC-MSCs and hESC-MSCs

Wenchuan Chen[a,b], **Xian Liu**[a,b], **Qianmin Chen**[a], **Chongyun Bao**[a,b], **Liang Zhao**[b,c], **Zhimin Zhu**[a], and **Hockin H.K. Xu**[b,d,e]

[a]State Key Laboratory of Oral Diseases, West China School of Stomatology, Sichuan University, Chengdu, Sichuan 610041, China

[b]Biomaterials & Tissue Engineering Division, Department of Endodontics, Periodontics and Prosthodontics, University of Maryland School of Dentistry, Baltimore, MD 21201, USA

[c]Department of Orthopaedic Surgery, Nanfang Hospital, Southern Medical University, Guangzhou, Guangdong 510515, China

[d]Center for Stem Cell Biology and Regenerative Medicine, University of Maryland School of Medicine, Baltimore, MD 21201, USA

[e]University of Maryland Marlene and Stewart Greenebaum Cancer Center, University of Maryland School of Medicine, Baltimore, MD 21201, USA

[f]Department of Mechanical Engineering, University of Maryland at Baltimore County, Baltimore County, MD 21250, USA

Abstract

Angiogenesis is a limiting factor in regenerating large bone defects. The objective of this study was to investigate angiogenic and osteogenic effects of coculture on calcium phosphate cement (CPC) scaffold using human umbilical vein endothelial cells (hUVECs) and mesenchymal stem cells (MSCs) from different origins for the first time. hUVECs were cocultured with four types of cells: human umbilical cord MSCs (hUCMSCs), human bone marrow MSCs (hBMSCs), and MSCs from induced pluripotent stem cells (hiPSC-MSCs) and embryonic stem cells (hESC-MSCs). Constructs were implanted in 8-mm cranial defects of rats for 12 weeks. CPC without cells served as control 1. CPC with hBMSCs served as control 2. Microcapillary-like structures were successfully formed on CPC *in vitro* in all four cocultured groups. Microcapillary lengths increased with time ($p<0.05$). Osteogenic and angiogenic gene expressions were highly elevated, and mineralization by cocultured cells increased with time ($p<0.05$). New bone amount and blood vessel density of cocultured groups were much greater than controls ($p<0.05$) in an animal study. hUVEC coculture with hUCMSCs, hiPSC-MSCs and hESC-MSCs achieved new bone and vessel

Correspondence: Dr. Hockin Xu, Department of Endodontics, Periodontics and Prosthodontics, University of Maryland Dental School, Baltimore, MD 21201 (hxu@umaryland.edu); Dr. Zhimin Zhu, West China School of Stomatology, Sichuan University, China (zzhimin@163.com); Dr. Liang Zhao, Department of Orthopaedic Surgery, Nanfang Hospital, Southern Medical University, Guangzhou, Guangdong 510515, China (lzhaonf@126.com).

No conflict of interest.

density similar to hUVEC coculture with hBMSCs ($p>0.1$). Therefore, hUCMSCs, hiPSC-MSCs and hESC-MSCs could serve as alternative cell sources to hBMSCs which require an invasive procedure to harvest. In conclusion, this study showed for the first time that cocultures of hUVECs with hUCMSCs, hiPSC-MSCs, hESC-MSCs and hBMSCs delivered via CPC scaffold achieved excellent osteogenic and angiogenic capabilities *in vivo*. The novel coculture constructs are promising for bone reconstruction with improved angiogenesis for craniofacial/orthopedic applications.

Keywords

Endothelial cell coculture; hBMSCs; hUCMSCs; hiPSC-MSCs; hESC-MSCs; angiogenesis/bone regeneration *in vivo*

1. Introduction

The need for regenerative medicine has increased as the population ages. Extensive efforts have been made to improve tissue repair and regeneration (Johnson et al., 2007; Silva et al., 2007; Mao et al., 2012; Boekhoven and Stupp, 2014; Abbott and Kaplan, 2015; Mikos et al., 2015; Pacheco et al., 2015; Shafiee and Atala, 2016). Bone tissue engineering approaches including stem cells and scaffolds are being developed as an exciting alternative to autogenous bone grafts (Mao et al., 2006; Link et al., 2008; Sundelacruz and Kaplan, 2009; Bohner, 2010; Ginebra et al., 2010; Saiz et al., 2013; Smith et al., 2015; Stoppel et al., 2015). However, for the reconstruction of large skeletal defects, bone engineering is limited by the inability to adequately vascularize (Klenke et al., 2008). The lack of a vasculature in tissue engineered constructs could result in inadequate oxygen and nutrition supply and waste removal, leading eventually to hypoxia and cell death. Thus, a functional microvasculature (angiogenesis) in bone engineered constructs is vital for successful therapeutic outcome in bone regeneration (Carano and Filvaroff, 2003). Several approaches were proposed to achieve rapid and sufficient angiogenesis (Hosseinkhani et al., 2006; Leach et al., 2006; Rouwkema et al., 2006; Unger et al., 2007; Rouwkema et al., 2008; Lovett et al., 2009; Santos et al., 2009; Wernike et al., 2010). They include the application of angiogenic growth factors to induce angiogenesis (Hosseinkhani et al., 2006; Leach et al., 2006; Rouwkema et al., 2008; Lovett et al., 2009; Wernike et al., 2010), and the creation of microvascular networks on biomaterials *in vitro* before implantation (prevascularization) (Rouwkema et al., 2006; Unger et al., 2007; Rouwkema et al., 2008; Lovett et al., 2009; Santos et al., 2009).

Angiogenesis involves the recruitment of endothelial cells (ECs) and other cells to develop capillaries and vessels (Gruber et al., 2005). Prevascularization of scaffolds was achieved with the coculture of ECs and osteoblasts (Unger et al., 2007; Santos et al., 2009). Coculture of ECs and osteoblasts on biomaterials produced a tissue-like self-assembly of cells with ECs forming microcapillary-like structures (Unger et al., 2007; Santos et al., 2009). Calcium phosphates are important for bone repair due to their excellent bioactivity and similarity to bone minerals (Grover et al., 2008; Liu et al., 2008; Liao et al., 2011; Houmard et al., 2012; Butscher et al., 2013; Ventura et al., 2014; Danoux et al., 2015; Pastorino et al., 2015). Our

recent study obtained microcapillary-like structures on calcium phosphate cement (CPC) scaffold via the coculture of ECs and osteoblasts (Xu and Thein-Han, 2013). However, osteoblasts might not be a good source of transplanted cells because they are not multipotent. Human bone marrow-derived mesenchymal stem cells (hBMSCs) can differentiate into osteoblasts, chondrocytes, adipocytes, and myoblasts, and are beneficial for bone regeneration (Petite et al., 2000) and angiogenesis (Au et al., 2008). Therefore, hBMSCs are considered the gold standard and are the most common cell source for bone regeneration (Petite et al., 2000; Au et al., 2008). However, the self-renewal and proliferative ability of hBMSCs decrease due to patient aging and diseases such as osteoporosis and arthritis.

Therefore, the old patients who need bone regeneration treatments may not be able to provide autologous hBMSCs for themselves. Hence, it is important to explore other types of stem cells for regenerative medicine. Recently, human umbilical cord MSCs (hUCMSCs) (Chen et al., 2012, 2012), human induced pluripotent stem cell-derived MSCs (hiPSC-MSCs) (Liu et al., 2013; Wang et al., 2014), and human embryonic stem cell-derived MSCs (hESC-MSCs) (Tang et al., 2012; Chen et al., 2013) have gained interest in stem cell and tissue regeneration research in combination with biomaterial scaffolds.

CPC has injectability, biocompatibility and osteoconductivity (Link et al., 2008; Bohner, 2010). However, limited angiogenesis and thus insufficient bone formation was observed with this material (Wernike et al., 2010). Prevascularization *in vitro* was promising to overcome this problem (Rouwkema et al., 2008; Lovett et al., 2009). This can potentially be achieved via the co-culture of ECs and osteoprogenitor cells (Rouwkema et al., 2006; Unger et al., 2007; Santos et al., 2009). Osteoblasts were cocultured with ECs to yield a tissue-like self-assembly of cells with ECs forming microcapillary-like structures (Xu and Thein-Han, 2013). However, a literature search revealed no report on the prevascularization of CPC via coculture of ECs and MSCs. Furthermore, to date, there has been no report on the comparison of endothelial cell coculture with hBMSCs, hUCMSCs, hiPSC-MSCs and hESC-MSCs to investigate the differences in angiogenic and osteogenic efficacy *in vivo*. Hence, the aim of this study was to investigate the angiogenic and osteogenic effects of coculture on macroporous and biofunctionalized CPC of human umbilical vein endothelial cells (hUVECs) with hBMSCs, hUCMSCs, hiPSC-MSCs and hESC-MSCs for the first time. It was hypothesized that: (1) Coculture of hUVECs with MSCs will undergo angiogenic and osteogenic differentiation and prevascularize the scaffold; (2) Cocultured constructs will produce significantly more new bone and vessels *in vivo* than the monoculture of hBMSCs; (3) hUVEC coculture with hUCMSCs, hiPSC-MSCs and hESC-MSCs will match the new bone and blood vessel regeneration of hUVEC coculture with the gold-standard hBMSCs.

2. Materials and methods

2.1 Fabrication of macroporous and biofunctionalized CPC

Macroporous and biofunctionalized CPC was made from CPC powder, CPC liquid and gas-foaming porogen following a previous study (Chen et al., 2013). The CPC powder consisted of an equimolar mixture of tetracalcium phosphate (TTCP: $Ca_4[PO_4]_2O$) and dicalcium

phosphate anhydrous (DCPA: $CaHPO_4$). The CPC liquid consisted of RGD-chitosan mixed with distilled water at a chitosan/(chitosan + water) mass fraction of 7.5%. RGD-chitosan was synthesized by coupling G4RGDSP (Thermo Fisher) with chitosan malate (chitosan; Vanson, Redmond, WA) following a previous study (Chen et al., 2013). Following another study (Chen et al., 2012), sodium hydrogen carbonate ($NaHCO_3$) and citric acid monohydrate ($C_6H_8O_7{\cdot}H_2O$) were added into CPC as a gas-foaming porogen. $NaHCO_3$ was added to CPC powder, at $NaHCO_3$/($NaHCO_3$ + CPC powder) mass fraction of 15%, as in a previous study (Chen et al., 2012). A corresponding amount of $C_6H_8O_7{\cdot}H_2O$ was added to CPC liquid, to maintain a $NaHCO_3$/($NaHCO_3$ + $C_6H_8O_7{\cdot}H_2O$) mass fraction of 54.52% (Hesaraki et al., 2008). CPC powder was mixed with CPC liquid at a powder to liquid mass ratio of 2 to 1. The paste was placed in a mold of 8 mm diameter and 1 mm thickness. CPC was incubated in a humidor with 100% relative humidity for 24 h at 37 °C. The CPC disks were sterilized in an ethylene oxide sterilizer (Andersen, Haw River, NC) for 12 h and then degassed for 7 d following the manufacturer's instructions.

2.2 hiPSCs, hESCs, hUCMSCs, hBMSCs and hUVECs culture and seeding on CPC

hiPSCs, hESCs, hUCMSCs, hBMSCs and hUVECs were used in this study. Their usage was approved by University of Maryland Institutional Review Board. hiPSCs were reprogrammed from adult bone marrow CD34+ cells and generously provided by Dr. Linzhao Chen at the Johns Hopkins University. MSCs were derived from the hiPSCs (hiPSC-MSCs) as described previously (Liu et al., 2013). Briefly, undifferentiated hiPSC were cultured as colonies on a feeder layer of mitotically-inactivated murine embryonic fibroblasts. The colonies were dissociated into clumps and induced to form floating embryoid bodies (EBs). After EBs were transferred into Nunclon Δ Surface six-well plates (Nunc, Rochester, NY) and adhered, many cells migrated out from the edges of the EBs. The outgrowth of cells were isolated by using cell scrapers and subcultured. The differentiated cells derived from these culture conditions were termed hiPSC-MSCs and cultured in MSC growth media. Our previous study (Liu et al., 2013) confirmed that the hiPSC-MSCs generated from this method expressed surface markers of MSCs (CD29, CD44, CD166, CD73), and were negative for typical hematopoietic (CD34), endothelial (CD31) and pluripotent markers (TRA-1-81 and OCT 3/4). These iPSC-MSCs were able to differentiate into three characteristic mesenchymal lineages including osteoblasts, adipocytes and chondrocytes (Liu et al., 2013).

hESCs were obtained from Wicell (H9, Madison, WI). Undifferentiated hESCs at passage 36 were cultured as colonies on a feeder layer of mitotically inactivated murine embryonic fibroblasts (MEF) (Tang et al., 2012; Chen et al., 2013). Aggregates were dissociated into clumps and cultured on 25 cm^2 ultra-low attachment culture flasks (Corning, Corning, NY) to form EBs. The EBs were transferred into six-well plates for further culture, and cells were sprouted and migrated out of the EBs spontaneously. These outgrowth cells were isolated by using cell scrapers and cultured in MSC growth medium. These MSCs were termed hESC-MSCs. These cells were characterized in our previous studies via flow cytometry, and the MSC surface markers were consistently and highly expressed (Tang et al., 2012; Chen et al., 2013). The MSC surface markers CD29, CD44, CD73, and CD166 were expressed to levels > 99.4%. On the other hand, the expressions of hematopoietic markers (CD31, CD34,

CD45) were less than 1.5%. Furthermore, HLA-ABC was expressed at 94.1%, whereas HLA-DR, TRA-1-81 and Oct3/4 were absent, which is characteristic for MSCs (Tang et al., 2012; Chen et al., 2013).

hUCMSCs were obtained from Lonza (Walkersville, MD) and cultured in MSC growth media, including low-glucose Dulbecco's modified Eagle's medium (DMEM) with 10% fetal bovine serum (FBS) and 1% penicillin/streptomycin (PS) (Invitrogen, Carlsbad, CA). hBMSCs (Lonza) were cultured in hBMSC growth medium, which consisted of DMEM plus 10% FBS, 1% PS, 0.25% gentamicin and 0.25% fungizone (Invitrogen). hUVECs (Lonza) were cultured in endothelial cell growth medium-2 (EGM-2; Lonza) consisting of endothelial cells basal medium-2 (EBM-2; Lonza) and a provided kit (Lonza) in a humidified incubator (5% CO_2, 37 °C) following a previous study (Xu and Thein-Han, 2013).

At 80% to 90% confluence, all four types of MSCs were detached by trypsin-EDTA (Invitrogen) and passaged. Passage 4 MSCs were osteogenically induced in osteogenic media for 2 weeks before being cocultured with hUVECs. The osteogenic media consisted of the MSC growth media supplemented with 100 nM dexamethasone, 10 mM β-glycerophosphate, 0.05 mM ascorbic acid, and 10 nM 1α, 25-Dihydroxyvitamin D3 (Sigma, St. Louis, MO).

hUVECs were mixed with each osteogenically-induced MSCs at hUVECs:MSCs of 4:1 ratio in EGM-2 culture medium for coculture (Santos et al., 2009). The macroporous CPC disks were pre-incubated with EGM-2 for 3 h in a humidified incubator prior to cell seeding. Then, they were placed individually in 12-well petri plate. Mixed hUVECs-MSCs suspension (1.5×10^5 cells/disk) was seeded drop-wise on the top of CPC scaffold disk and cultured with EGM-2 in a humidified incubator (5% CO_2, 37 °C) for 2, 4 and 6 weeks, respectively, to examine vascular formation on CPC scaffold (Santos et al., 2009).

2.3 Immunofluorescent staining of PECAM -1 (CD31)

To determine vascular formation, cell-scaffold constructs were immunofluorescently stained for PECAM-1 (CD31, endothelial-specific) (Invitrogen) at 2, 4 and 6 weeks. The samples were rinsed with phosphate-buffered saline (PBS), fixed with 4% parformaldehyde for 20 min, washed with PBS, permeabilized with 0.5% Triton X-100 for 5 min, which could help expose epitopes of the proteins (Hsu and Youle, 1998), and blocked with 0.1% bovine serum albumin (BSA) for 30 min. After washing with PBS, the samples were incubated with primary mouse monoclonal antibody anti-human CD31 (1:200, Invitrogen) overnight at 4 ˚C. The samples were washed with PBS and incubated with secondary antibody (1:1000, goat anti-mouse Alexa Fluor 488, green fluorescence, Invitrogen) for 1 h. This was followed by rinsing in PBS, staining of the nuclei with DAPI (1 μg/mL, Sigma) for 10 min and washing with PBS. The samples were then placed in Fluoromount Aqueous Mounting Medium (Sigma) and examined with epifluorescence microscopy (TE2000S, Nikon, Melville, NY). This method stained hUVECs in green color as tube-like or microcapillary-like structures. Three random fields of view were imaged from each of five samples (yielding 15 photos for each MSC cell type at each time period). The lengths of microcapillaries weres measured with Image-Pro Plus software (Media Cybernetics, Silver

Springs, MD) to obtain the cumulative length of microcapillaries for each image. The cumulative length of microcapillaries of the image was divided by the area of that image, to yield the cumulative microcapillary length per scaffold surface area (Chen et al., 2014).

2.4 Quantitative real time-PCR

At 2, 4, 6 weeks, quantitative real-time polymerase chain reaction (qRT-PCR, 7900HT, Applied Biosystems, Foster City, CA) was used to measure gene expressions of the cocultured cells on CPC-RGD. The total cellular RNA of the cocultured cells was extracted with TRIzol reagent (Invitrogen). RNA was reverse-transcribed into cDNA using a High-Capacity cDNA reverse transcription kit (Applied Biosystems). Gene expressions were measured by TaqMan gene expression kits, including human alkaline phosphatase (ALP, Hs00758162_m1), osteocalcin (OC, Hs00609452_g1), collagen type I (Coll I, Hs00164004), vascular endothelial growth factor A (VEGF) (HS00900055_ml), vascular endothelial cadherin (VE-cadherin) (Hs00170986_m1), von-Willebrand factor (vWF) (Hs00169795_m1), and glyceraldehyde 3-phosphate dehydrogenase (GAPDH, Hs99999905). The $2^{-\Delta\Delta Ct}$ method was used to evaluate the relative expression for each target gene (Chen et al., 2014). The C_t of target genes was normalized by the C_t of the housekeeping gene GAPDH to obtain ΔC_t. The C_t value of coculture on tissue culture polystyrene for 1 d served as the calibrator.

2.5 Mineral synthesis by cocultured cells

At 2, 4 and 6 weeks, CPC disks with cocultured cells were washed with PBS, fixed with 10% formaldehyde, and stained with Alizarin Red S (ARS, Millipore, Billerica, MA) for 20 min. ARS stains calcium-rich deposits synthesized by cells into a red color (Chen et al., 2012, 2013). An osteogenesis assay (Millipore) was used to extract the stained minerals and measure the ARS concentration at OD_{405}, following the manufacturer's instructions. The ARS standard curve was made with known concentration of the dye. CPC disks without cells (control) were also measured at the same time periods. The ARS concentration of control was subtracted from that of cell-seeded disks to yield the net mineral concentration synthesized by cells (Chen et al., 2012, 2013).

2.6 Animal experiment and surgical procedures

The following six groups were tested in rats:

1. CPC scaffold seeded with hUCMSCs and hUVECs coculture (referred to as UCM-EC);
2. CPC scaffold seeded with hiPSC-MSCs and hUVECs coculture (referred to as iPM-EC);
3. CPC scaffold seeded with hESC-MSCs and hUVECs coculture (referred to as ESM-EC);
4. CPC scaffold seeded with hBMSCs and hUVECs coculture (referred to as BM-EC);
5. CPC scaffold without cells (Control 1);

6. CPC scaffold with monocultured hBMSCs, no hUVEC coculture (Control 2).

Groups 1–4 were cocultured in EGM-2 and Groups 5–6 were cultured in osteogenic media for 4 weeks prior to implantation in rats. The critical-sized cranial defect model in rats was approved by University of Maryland (IACUC # 0909014) (Chen et al., 2013). All procedures followed NIH animal care guidelines. Athymic nude rats (200–250 g, 7–8 weeks old) (Harlan, Indianapolis, IN) were anesthetized by intraperitoneal injection with a combination of 75 mg/kg body weight (b.w.) of ketamine and 10 mg/kg b.w. of xylazine. The cranium was shaved and iodinated before fixation. Surgery was performed under aseptical conditions. A midlongitudinal incision of 2 cm was made on the dorsal surface of the cranium, and the periosteum was completely cleared by scraping. A trephine bur was used to create a circular defect of 8 mm diameter in the cranium (Chen et al., 2013). The full thickness of the cranial bone in the circular defect was removed under constant irrigation with sterile saline. The defect was implanted with one of the six groups, the defect was closed and the soft tissues were sutured. For CPC with cells, the constructs were implanted with the cell-seeded surface contacting the dura of the rats. Twelve weeks after surgery, five rats from each group were euthanized with carbon dioxide, and the implants embedded in the surrounding native bone were retrieved (Chen et al., 2013). The implants were fixed for 24 h at 4 °C in 10% zinc-buffered formalin and analyzed by histology.

2.7 Histological and histomorphological analysis

The retrieved implant specimens were decalcified in 30% buffered formic acid at room temperature for 1 week. Specimens were embedded in paraffin and the central part of the defect with implant was cut into 5 μm thick sections (Chen et al., 2013). Paraffin sections were stained with hematoxylin/eosin (HE), and the histologic images of the sections were analyzed by the software Image Pro Plus (Media Cybernetics, Carlsbad, CA). The perimeter around the new bone was traced, and the area of the new bone was measured by the software (Chen et al., 2013). New bone area fraction was calculated as the new bone area/the entire defect area. Blood vessels were identified by their luminal structure and the presence of red blood cells within their boundaries (Kaigler et al., 2005; Chen et al., 2016). New vessel density was determined as the number of blood vessels per area of the defect. One section from the central part of the implant for each rat was analyzed and the average value was obtained for each group (n = 5).

2.8 Statistical Analyses

Statistical analyses were performed using Statistical Package for the Social Sciences (SPSS 16.0, Chicago, IL, USA). Statistical significance was calculated by using multi-way analysis of variance (ANOVA). Statistical significance was defined as $p < 0.05$.

3. Results

Coculturing hUVECs with various types of MSCs on CPC scaffold *in vitro* and formation of microcapillary-like structures are shown in Fig. 1: (A–D) Immunofluorescent images, (E) cumulative vessel length (mean ± sd; n = 5). By immunostaining for endothelial marker PECAM1, hUVECs were identified by green fluorescence on the cell membranes. They showed typical cobblestone-like morphology of epithelial cells. Nuclear counterstaining

with DAPI in blue was used to detect all cells, including MSCs which were without the green staining. Epifluorescence microscopy showed microcapillary-like structures on all constructs at 2 weeks (not shown). At 4 weeks, more microcapillary-like structures were observed on all constructs (not shown). At 6 weeks, representative microcapillary-like structures are shown in Fig. 1A–D. The branches and interconnections of microcapillary-like structures increased with culture time. This was quantified in Fig. 1E. All four MSC types in coculture with hUVECs produced similar lengths of microcapillary-like structures ($p > 0.1$).

The expressions of three osteogenic differentiation genes (ALP, OC, and COL I) and three angiogenic genes (VEGF, VE-cadherin, and vWF) are shown in Fig. 2 (mean ± sd; $n = 5$). All the cocultured cells showed osteogenic differentiation, indicated by highly elevated ALP, OC and COL I peaks, compared to control value which was set at 1. For all groups, ALP peaked at 2 weeks, OC peaked at 4 weeks, and COL I peaked at 2 weeks. For angiogenic expressions, VEGF was greatly up-regulated over the control value of 1, and it had an increasing trend with time, peaking at 4 or 6 weeks. The VE-cadherin expression significantly increased and peaked at 4 weeks. The vWF expression decreased from 2 to 6 weeks ($p < 0.05$), with expressions less than the control value of 1.

The cell-synthesized mineral results are shown in Fig. 3: (A) Representative ARS staining images at 6 weeks, and (B) data from the osteogenesis assay (mean ± sd; $n = 5$). In (A), coculture of hUVECs with hUCMSCs, hiPSC-MSCs, hESC-MSCs and hBMSCs on CPC scaffold yielded bone minerals. ARS staining yielded a thick and dense red layer of new mineral matrix synthesized by the cocultured cells covering the scaffold at 6 weeks. In (B), the cell-synthesized mineral amount significantly increased from 2 to 6 weeks ($p< 0.05$). At each time period, coculture of hUVECs with hUCMSCs, hiPSC-MSCs, hESC-MSCs or hBMSCs had no significant difference in mineral synthesis ($p > 0.1$).

Representative histological H&E staining images at 12 weeks in rats are shown in Fig. 4 for the six groups tested. There were no significant signs of inflammation or immunologic response in any groups. New bone formation is indicated by the arrows. New bone formed along scaffold surfaces especially at the dura side, as well as in the interior of the scaffold likely due to macropores. Examination of all samples for all groups indicated that new bone amounts of the four cocultured groups were similar, and all had noticeably more new bone than control 1 without cells and control 2 with only hBMSCs.

High magnification examples of new bone formation are shown in Fig. 5 for BM+EC group at 12 weeks. In (A) the appearance of osteoid with osteocytes and blood vessels are visible, as well as newly-formed bone lined by osteoblasts. Typical examples of CPC material loss and resorption are shown in (B). CPC was resorbed and replaced by new bone. Osteoclast-like multinuclear giant cells were observed that contribute to CPC resorption.

The quantitative bone regeneration results are plotted in Fig. 6: (A) New bone area fraction, and (B) blood vessel density (mean ± sd; $n = 5$). The amount of new bone was the smallest for control 1, which used CPC scaffold without cells. Approximately two times of new bone was formed in control 2, which used CPC with hBMSCs. The four coculture groups caused

another 35% increase in new bone over control 2 ($p < 0.05$). New blood vessel density showed a similar increasing trend from control 1 to control 2 to coculture ($p < 0.05$).

4. Discussion

This study investigated the coculture of hUVECs with hUVMSCs, hiPSC-MSCs, hESC-MSCs and hBMSCs in macroporous CPC-RGD scaffold for angiogenic and osteogenic regeneration *in vivo* for the first time. This study demonstrated that the coculture of hUVECs with MSCs from different origins all underwent successful angiogenic and osteogenic differentiation and prevascularized the CPC scaffold. The novel cocultured constructs produced greater new bone amount and vessel density *in vivo* than the monoculture of hBMSCs without coculture. In addition, the hUVEC coculture with hUCMSCs, hiPSC-MSCs and hESC-MSCs all matched the new bone amount and blood vessel density of hUVEC coculture with the gold-standard hBMSCs. These results indicate that (1) hUCMSCs, hiPSC-MSCs and hESC-MSCs are good alternative cell sources to hBMSCs which requires an invasive procedure to harvest and may lose potency due to patient aging and diseases; (2) the novel constructs with coculture of hUVECs with MSCs in CPC are promising for bone regeneration applications with enhanced bone and blood vessel formations.

An ideal scaffold for bone regeneration should serve as a template for cell attachment, growth, differentiation and vascularization, and ultimately be replaced by new bone *in vivo*. CPC has good biocompatibility, osteoconductivity and bone replacement capability. The incorporation of angiogenic growth factors in CPC and the creation of microvascular networks in CPC prior to implantation were previously studied to address the issue of limited angiogenesis and thus insufficient bone formation (Wernike et al., 2010; Chen et al., 2014). However, a literature search revealed no report on the investigation of coculture of ECs with different types of MSCs on bone regeneration efficacy.

A rapid formation of functional blood vessels is crucial for the survival of biomaterials after implantation *in vivo*. For bone vascularization approaches in tissue engineering, ECs have attracted much attention due to their unique role in angiogenesis. However, ECs cannot complete vessel formation on their own, because extracellular matrix and mesenchymal cells also play important roles in angiogenesis. The cross-talk and interactions between ECs and osteoblast-like cells (such as primary osteoblasts and osteoblastic-cell lines) are critical for osteogenesis during embryonic development as well as for bone repair and regeneration after injury (Deckers et al., 2002; Villars et al., 2002; Brandi and Collin-Osdoby, 2006). Therefore, the coculture of ECs with osteoblasts has been a proposed strategy for both angiogenesis and osteogenesis. There were some models of cocultured ECs with osteoblast-like cells resulting in the formation of vessel-like structures similar to those observed *in vivo* (Wenger et al., 2004; Rouwkema et al., 2006; Fuchs et al., 2007; Santos et al., 2009; Chen et al., 2014). MSCs have properties of self-renewal, multipotent differentiation, homing, and immunomodulatory activity. MSCs are typically adult stem or progenitor cells and they can be isolated from a number of tissues in the body. They show greater proliferative capacity and differentiation potential than terminally differentiated cells; hence, MSCs likely are superior to osteoblasts. In addition, the interactions between MSCs and ECs could regulate

each other's activities. On one hand, ECs and the matrix have significant influence on the differentiation of MSCs (Lozito et al., 2009; Saleh et al., 2011). On the other hand, MSCs could promote the biological functions of ECs by inhibiting apoptosis, increasing the survival, promoting migration and stimulating angiogenesis of the cells (Hung et al., 2007; Zhang et al., 2012). Therefore, MSCs are increasingly thought to be part of a perivascular niche. Nevertheless, to date, there has been no report that investigated coculture systems including the use of ECs with hiPSC-MSCs or hESC-MSCs; in particular, there has been no comparison on different types of MSCs in coculture on bone regeneration. Hence, cocultures of ECs with MSCs of different origins were investigated in the present study which successfully formed vascular structures on CPC scaffold. It should be noted that cumulative microcapillary length per scaffold surface area was measured in the present study. This parameter is different from the density of vascular structure. This is because in three-dimensional tissues, the capillaries are three-dimensionally distributed; when the tissue is sectioned into a two-dimensional slide, it can be used to count the number of capillaries to yield the density of vasculature. However, the vascular structure in the present study was formed on the CPC surface and was tube-like and interconnected on the same surface. Therefore, it was not possible to count the individual vascular numbers; hence the cumulative vascular length in the immunofluorescent image was measured in vitro. For the in vivo specimens in the present study, blood vessels were counted from H and E stained tissue sections, following previous studies (Kaigler et al., 2005; Chen et al., 2016). Further study should immune-label the vessels and then count them based on immunostaining and morphological characteristics.

PECAM-1 (cluster of differentiation 31, CD31) is normally found on the surface of ECs and primarily used to demonstrate the distribution of ECs (Chen et al., 2014). In the present study, ECs were shown by staining of PECAM-1 to form microcapillary-like structures in all cocultured constructs; hence, all four types of MSCs could support the microcapillary-like structure formation by ECs. Little is known about the mechanism of microcapillary-like structure self-assembly on biomaterials. However, it is known that many growth factors are produced by ECs and MSCs to affect the growth and differentiation of the reciprocal cells (Unger et al., 2015), which likely makes the cocultured cells to differentiate into more than the two original types of cells. Therefore, in the present study, the cocultured cells were not removed from the macroporous and rough CPC surfaces to separate them into the two original types of cells to measure their respective gene expressions. While performing the separation of different cell types before PCR analysis is meritorious, it was not done in the present study because of the following reasons. First, both MASC technology and flow cytometry require single suspension cells, but it was difficult to remove and retrieve intact cells from the macroporous and rough CPC scaffold surfaces. Second, after being cocultured, the cells might have differentiated into more than the two original types of cells, thus it would be difficult to separate them back into the two original types of cells. Third, similar to the measurement of gene expressions of tissues with many types of cells, by considering the same expression amounts of the house-keeping gene, the cocultured cells at 1 day were used as the calibrator to enable the evaluation of the total gene expression of the cocultured cells at different time points in the present study.

All four types of MSCs on the scaffolds successfully went into the osteogenic differentiation pathway, with high expressions of osteogenic markers (ALP, OC, and COL I). The ECs in all the four cocultured constructs underwent angiogenic differentiation, with high expressions of VE-cadherin (Chen et al., 2014), which is indispensable for proper vascular morphogenesis and serves the purpose of maintaining the newly-formed vessels. ECs in all the four cocultured constructs decreased the expression of vWF (Chen et al., 2014), which indicates an increase in angiogenesis and vessel formation. Since the increased VEGF produced by osteogenic cells is one of the most important pro-angiogenic factors with well-established actions on ECs, the high amount of VEGF may contribute to microcapillary-like structure formation (Chen et al., 2014). In addition, under hypoxia, MSCs showed an increased synthesis and secretion of several cytokines which can inhibit the apoptosis of ECs and accelerate angiogenesis (Gnecchi et al., 2005; Hung et al., 2007). Therefore, the ability of MSCs to alter the tissue microenvironment (improving the niche) via secretion of soluble factors may contribute more significantly than their capacity for transdifferentiation in tissue repair (Hung et al., 2007). Furthermore, the attachment of hUVECs on the scaffold may also be enhanced by the attachment and spreading of the MSCs and by their matrix production (Unger et al., 2015). In addition, COL I can mediate cell adhesion, contribute to the mature osteoblast phenotype, provide template for mineralization, and drive EC migration (Pham et al., 2008). Therefore, the deposit of an extensive network of COL I by MSCs in the scaffold can provide an essential 3D support for ECs to migrate and organize into microcapillary-like structures. Cell attachment on scaffold can be further improved by the immobilization of RGD (Chen et al., 2014). The improved adhesion of cells may be beneficial for matrix production by MSCs and for the migration of hUVECs. These factors likely helped enable the hUVECs to migrate within the matrix to form the observed extensive microcapillary-like structures.

hUCMSCs are inexpensive and inexhaustible, and have been shown to possess a high plasticity and developmental flexibility (Can and Karahuseyinoglu, 2007; Chen et al., 2013). hUCMSCs caused no immunorejection in preliminary studies and were not known to be tumorigenic (Can and Karahuseyinoglu, 2007). Therefore, hUCMSCs could be highly beneficial for bone regeneration. hESCs are relatively homogenous, possess great proliferation to provide an unlimited MSCs (hESC-MSCs), and can be differentiated into all cell types, including bone-forming cells. In addition, hiPSCs are autogeneically accessible and have nearly unlimited potential to proliferate and differentiate into all derivatives of the three germ layers. These advantages make hUCMSCs, hESC-MSCs and hiPSCs-MSCs attractive alternatives to hBMSCs for bone regeneration. These alternative cell sources are valuable because hBMSCs require an invasive procedure to harvest which yields only limited cell numbers. In addition, hBMSCs from seniors and those patients with various diseases may not be sufficiently potent for tissue regeneration, hence the alternative cell sources may be especially needed for these patients.

The four cell types, hUCMSCs, hiPSC-MSCs, hESC-MSCs and hBMSCs, were cocultured with hUVECs and compared for bone and blood vessel regeneration in the present study. The four cocultured constructs had similar results in the following five aspects of analysis: Amount of microcapillary-like structure formation, expression patterns of osteogenic and angiogenic differentiation genes, amount of mineral synthesis *in vitro*, and *in vivo* new bone

amount and blood vessel density. Furthermore, the macroporous CPC scaffold with cocultures of ECs and MSCs exhibited an increased osteogenic and angiogenic capacity, compared to scaffold with only hBMSCs. These results demonstrated that the cocultures of ECs and MSCs were more committed to osteogenesis and angiogenesis than MSCs alone, and the four types of MSCs had similar osteogenic capacity and supported prevascularization *in vitro* and angiogenesis *in vivo*. Therefore, (1) hUCMSCs, hiPSC-MSCs and hESC-MSCs could be valuable alternatives to hBMSCs in enhancing bone and blood vessel regeneration to a similar extent; (2) the coculture of hUVECs with hUCMSCs, hiPSC-MSCs, hESC-MSCs and hBMSCs all had greater new bone and vessel density than hBMSCs alone; and (3) macroporous CPC-RGD was a suitable scaffold to deliver cocultures of hUVECs with MSCs for bone regeneration. In the present study, the blood vessels in vivo were all formed in the scaffold area, hence they were all newly-formed vessels inside the defect. However, they could be formed both by the implanted cells and by the adjacent host cells. Further study should use cell-tracking to investigate the contribution of the implanted cells on vessel formation. Cell-tracking methods such as magnetic resonance imaging (MRI) (Srivastava et al., 2015), radionuclide imaging (Ding et al., 2004), antigen labelling (Sauerzweig et al., 2009), fluorescent protein labelling (Lippincott-Schwartz et al., 2003), fluorescent dye labelling (Kruyt et al., 2003), etc., could enable such a study. Further studies are also needed to investigate the effects of key parameters including cell seeding density and EC to MSC ratio, as well as bone and vessel regeneration in large animal models.

5. Conclusion

This study showed for the first time that hUVEC coculture with hUCMSCs, hiPSC-MSCs, hESC-MSCs and hBMSCs in CPC scaffold achieved excellent osteogenic and angiogenic capability *in vivo*. These findings indicate the feasibility of generating a prevascularized network on CPC scaffold, the benefits of cocultures of hUVECs with various types of MSCs to increase new bone and blood vessel formation, and the potential of using hUCMSCs, hiPSC-MSCs and hESC-MSCs as alternatives to the gold-standard hBMSCs in coculturing prevascularization and bone repair. The novel coculture constructs with stem cell delivery are promising for a wide range of dental, craniomaxillofacial and orthopedic applications to enhance vascularization and bone regeneration.

Acknowledgments

We are indebted to Prof. Linzhao Chen at Johns Hopkins University for providing the hiPSCs. We thank Drs. David J. Mooney, Michael D. Weir, Chen Chen, Ping Wang and Cindy Zhou for discussions and help. This study was supported by NIH R01 DE14190 and R21 DE22625 (HX), Natural Science Foundation of China NSFC 81000455 (WC), NSFC 31328008 (LZ), NSF Guangdong 20130010014253 (LZ) and 2014A030313275 (LZ), and the University of Maryland School of Dentistry bridge grant (HX).

References

Abbott RD, Kaplan DL. Strategies for improving the physiological relevance of human engineered tissues. Trends Biotechnol. 2015; 33:401–407. [PubMed: 25937289]

Au P, Tam J, Fukumura D, Jain RK. Bone marrow-derived mesenchymal stem cells facilitate engineering of long-lasting functional vasculature. Blood. 2008; 111:4551–4558. [PubMed: 18256324]

Boekhoven J, Stupp SI. 25th anniversary article: supramolecular materials for regenerative medicine. Adv Mater. 2014; 26:1642–1659. [PubMed: 24496667]

Bohner M. Design of ceramic-based cements and putties for bone graft substitution. Eur Cell Mater. 2010; 20:1–12. [PubMed: 20574942]

Brandi ML, Collin-Osdoby P. Vascular biology and the skeleton. J Bone Miner Res. 2006; 21:183–192. [PubMed: 16418774]

Butscher A, Bohner M, Doebelin N, Hofmann S, Müller R. New depowdering-friendly designs for three-dimensional printing of calcium phosphate bone substitutes. Acta Biomater. 2013; 9:9149–9158. [PubMed: 23891808]

Can A, Karahuseyinoglu S. Concise review: human umbilical cord stroma with regard to the source of fetus-derived stem cells. Stem Cells. 2007; 25:2886–2895. [PubMed: 17690177]

Carano RA, Filvaroff EH. Angiogenesis and bone repair. Drug Discov Today. 2003; 8:980–989. [PubMed: 14643161]

Chen WC, Liu J, Manuchehrabadi N, Weir MD, Zhu ZM, Xu HHK. Umbilical cord and bone marrow mesenchymal stem cell seeding on macroporous calcium phosphate for bone regeneration in rat cranial defects. Biomaterials. 2013; 34:9917–9925. [PubMed: 24054499]

Chen WC, Thein-Han W, Weir MD, Chen QM, Xu HHK. Prevascularization of biofunctional calcium phosphate cement for dental and craniofacial repairs. Dent Mater. 2014; 30:535–544. [PubMed: 24731858]

Chen WC, Zhou HZ, Tang MH, Weir MD, Bao CY, Xu HHK. Gas-foaming calcium phosphate cement scaffold encapsulating human umbilical cord stem cells. Tissue Eng Part A. 2012; 18:816–827. [PubMed: 22011243]

Chen WC, Zhou HZ, Weir MD, Bao CY, Xu HHK. Umbilical cord stem cells released from alginate-fibrin microbeads inside macroporous and biofunctionalized calcium phosphate cement for bone regeneration. Acta Biomater. 2012; 8:2297–2306. [PubMed: 22391411]

Chen WC, Zhou HZ, Weir MD, Tang MH, Bao CY, Xu HHK. Human embryonic stem cell-derived mesenchymal stem cell seeding on calcium phosphate cement-chitosan-RGD scaffold for bone repair. Tissue Eng Part A. 2013; 19:915–927. [PubMed: 23092172]

Chen Z, Wei J, Zhu J, et al. Chm-1 gene-modified bone marrow mesenchymal stem cells maintain the chondrogenic phenotype of tissue-engineered cartilage. Stem Cell Res Ther. 2016; 7:70. [PubMed: 27150539]

Danoux CB, Bassett DC, Othman Z, et al. Elucidating the individual effects of calcium and phosphate ions on hMSCs by using composite materials. Acta Biomater. 2015; 17:1–15. [PubMed: 25676583]

Deckers MM, van Bezooijen RL, van der Horst G, et al. Bone morphogenetic proteins stimulate angiogenesis through osteoblast-derived vascular endothelial growth factor A. Endocrinology. 2002; 143:1545–1553. [PubMed: 11897714]

Ding W, Bai J, Zhang J, et al. In vivo tracking of implanted stem cells using radio-labeled transferrin scintigraphy. Nucl Med Biol. 2004; 31:719–725. [PubMed: 15246362]

Fuchs S, Hofmann A, Kirkpatrick CJ. Microvessel-like structures from outgrowth endothelial cells from human peripheral blood in 2-dimensional and 3-dimensional co-cultures with osteoblastic lineage cells. Tissue Eng. 2007; 13:2577–2588. [PubMed: 17655487]

Ginebra MP, Espanol M, Montufar EB, Perez RA, Mestres G. New processing approaches in calcium phosphate cements and their applications in regenerative medicine. Acta Biomater. 2010; 6:2863–2873. [PubMed: 20123046]

Gnecchi M, He H, Liang OD, et al. Paracrine action accounts for marked protection of ischemic heart by Akt-modified mesenchymal stem cells. Nat Med. 2005; 11:367–368. [PubMed: 15812508]

Grover LM, Hofmann MP, Gbureck U, Kumarasami B, Barralet JE. Frozen delivery of brushite calcium phosphate cements. Acta Biomater. 2008; 4:1916–1923. [PubMed: 18657496]

Gruber R, Kandler B, Holzmann P, et al. Bone marrow stromal cells can provide a local environment that favors migration and formation of tubular structures of endothelial cells. Tissue Eng. 2005; 11:896–903. [PubMed: 15998229]

Hesaraki S, Zamanian A, Moztarzadeh F. The influence of the acidic component of the gas-foaming porogen used in preparing an injectable porous calcium phosphate cement on its properties: acetic

acid versus citric acid. J Biomed Mater Res B Appl Biomater. 2008; 86:208–216. [PubMed: 18161816]

Hosseinkhani H, Hosseinkhani M, Khademhosseini A, Kobayashi H, Tabata Y. Enhanced angiogenesis through controlled release of basic fibroblast growth factor from peptide amphiphile for tissue regeneration. Biomaterials. 2006; 27:5836–5844. [PubMed: 16930687]

Houmard M, Fu Q, Saiz E, Tomsia AP. Sol-gel method to fabricate CaP scaffolds by robocasting for tissue engineering. J Mater Sci Mater Med. 2012; 23:921–930. [PubMed: 22311079]

Hsu YT, Youle RJ. Bax in murine thymus is a soluble monomeric protein that displays differential detergent-induced conformations. J Biol Chem. 1998; 273:10777–10783. [PubMed: 9553144]

Hung SC, Pochampally RR, Chen SC, Hsu SC, Prockop DJ. Angiogenic effects of human multipotent stromal cell conditioned medium activate the PI3K-Akt pathway in hypoxic endothelial cells to inhibit apoptosis, increase survival, and stimulate angiogenesis. Stem Cells. 2007; 25:2363–2370. [PubMed: 17540857]

Johnson PC, Mikos AG, Fisher JP, Jansen JA. Strategic directions in tissue engineering. Tissue Eng. 2007; 13:2827–2837. [PubMed: 18052823]

Kaigler D, Krebsbach PH, West ER, Horger K, Huang YC, Mooney DJ. Endothelial cell modulation of bone marrow stromal cell osteogenic potential. FASEB J. 2005; 19:665–667. [PubMed: 15677693]

Klenke FM, Liu Y, Yuan H, Hunziker EB, Siebenrock KA, Hofstetter W. Impact of pore size on the vascularization and osseointegration of ceramic bone substitutes in vivo. J Biomed Mater Res A. 2008; 85:777–786. [PubMed: 17896777]

Kruyt MC, De Bruijn J, Veenhof M, et al. Application and limitations of chloromethyl-benzamidodialkylcarbocyanine for tracing cells used in bone. Tissue Eng. 2003; 9:105–115. [PubMed: 12625959]

Leach JK, Kaigler D, Wang Z, Krebsbach PH, Mooney DJ. Coating of VEGF-releasing scaffolds with bioactive glass for angiogenesis and bone regeneration. Biomaterials. 2006; 27:3249–3255. [PubMed: 16490250]

Liao H, Walboomers XF, Habraken WJ, et al. Injectable calcium phosphate cement with PLGA, gelatin and PTMC microspheres in a rabbit femoral defect. Acta Biomater. 2011; 7:1752–1759. [PubMed: 21185953]

Link DP, van den Dolder J, van den Beucken JJ, Wolke JG, Mikos AG, Jansen JA. Bone response and mechanical strength of rabbit femoral defects filled with injectable CaP cements containing TGF-beta 1 loaded gelatin microparticles. Biomaterials. 2008; 29:675–682. [PubMed: 17996293]

Lippincott-Schwartz J, Patterson GH. Development and use of fluorescent protein markers in living cells. Science. 2003; 300:87–91. [PubMed: 12677058]

Liu C, Chen CW, Ducheyne P. In vitro surface reaction layer formation and dissolution of calcium phosphate cement-bioactive glass composites. Biomed Mater. 2008; 3:034111. [PubMed: 18689928]

Liu J, Chen WC, Zhao ZH, Xu HHK. Reprogramming of mesenchymal stem cells derived from iPSCs seeded on biofunctionalized calcium phosphate scaffold for bone engineering. Biomaterials. 2013; 34:7862–7872. [PubMed: 23891395]

Lovett M, Lee K, Edwards A, Kaplan DL. Vascularization strategies for tissue engineering. Tissue Eng Part B Rev. 2009; 15:353–370. [PubMed: 19496677]

Lozito TP, Kuo CK, Taboas JM, Tuan RS. Human mesenchymal stem cells express vascular cell phenotypes upon interaction with endothelial cell matrix. J Cell Biochem. 2009; 107:714–722. [PubMed: 19415687]

Mao JJ, Giannobile WV, Helms JA, et al. Craniofacial tissue engineering by stem cells. J Dent Res. 2006; 85:966–979. [PubMed: 17062735]

Mao JJ, Robey PG, Prockop DJ. Stem cells in the face: tooth regeneration and beyond. Cell Stem Cell. 2012; 11:291–301. [PubMed: 22958928]

Mikos AG, Johnson PC, Fisher JP, Jansen JA. The Maturation of Tissue Engineering. Tissue Eng Part A. 2015; 21:2473–2475. [PubMed: 26402224]

Pacheco DP, Reis RL, Correlo VM, Marques AP. The crosstalk between tissue engineering and pharmaceutical biotechnology: recent advances and future directions. Curr Pharm Biotechnol. 2015; 16:1012–1023. [PubMed: 26306746]

Pastorino D, Canal C, Ginebra MP. Multiple characterization study on porosity and pore structure of calcium phosphate cements. Acta Biomater. 2015; 28:205–214. [PubMed: 26384703]

Petite H, Viateau V, Bensaid W, et al. Tissue-engineered bone regeneration. Nat Biotechnol. 2000; 18:959–963. [PubMed: 10973216]

Pham QP, Kasper FK, Scott BL, Raphael RM, Jansen JA, Mikos AG. The influence of an in vitro generated bone-like extracellular matrix on osteoblastic gene expression of marrow stromal cells. Biomaterials. 2008; 29:2729–2739. [PubMed: 18367245]

Rouwkema J, de Boer J, Van Blitterswijk CA. Endothelial cells assemble into a 3-dimensional prevascular network in a bone tissue engineering construct. Tissue Eng. 2006; 12:2685–2693. [PubMed: 16995802]

Rouwkema J, Rivron NC, van Blitterswijk CA. Vascularization in tissue engineering. Trends Biotechnol. 2008; 26:434–441. [PubMed: 18585808]

Saiz E, Zimmermann EA, Lee JS, Wegst UG, Tomsia AP. Perspectives on the role of nanotechnology in bone tissue engineering. Dent Mater. 2013; 29:103–115. [PubMed: 22901861]

Saleh FA, Whyte M, Ashton P, Genever PG. Regulation of mesenchymal stem cell activity by endothelial cells. Stem Cells Dev. 2011; 20:391–403. [PubMed: 20536359]

Santos MI, Unger RE, Sousa RA, Reis RL, Kirkpatrick CJ. Crosstalk between osteoblasts and endothelial cells co-cultured on a polycaprolactone-starch scaffold and the in vitro development of vascularization. Biomaterials. 2009; 30:4407–4415. [PubMed: 19487022]

Sauerzweig S, Baldauf K, Braun H, Reymann KG. Time-dependent segmentation of BrdU-signal leads to late detection problems in studies using BrdU as cell label or proliferation marker. J Neurosci Methods. 2009; 177:149–159. [PubMed: 19007815]

Shafiee A, Atala A. Printing Technologies for Medical Applications. Trends Mol Med. 2016; 22:254–265. [PubMed: 26856235]

Silva GA, Coutinho OP, Ducheyne P, Reis RL. Materials in particulate form for tissue engineering. 2. Applications in bone. J Tissue Eng Regen Med. 2007; 1:97–109. [PubMed: 18038398]

Smith BT, Shum J, Wong M, Mikos AG, Young S. Bone Tissue Engineering Challenges in Oral & Maxillofacial Surgery. Adv Exp Med Biol. 2015; 881:57–78. [PubMed: 26545744]

Stoppel WL, Ghezzi CE, McNamara SL, Black LD, Kaplan DL. Clinical applications of naturally derived biopolymer-based scaffolds for regenerative medicine. Ann Biomed Eng. 2015; 43:657–680. [PubMed: 25537688]

Srivastava AK, Kadayakkara DK, Bar-Shir A, Gilad AA, McMahon MT, Bulte JW. Advances in using MRI probes and sensors for in vivo cell tracking as applied to regenerative medicine. Dis Model Mech. 2015; 8:323–336. [PubMed: 26035841]

Sundelacruz S, Kaplan DL. Stem cell- and scaffold-based tissue engineering approaches to osteochondral regenerative medicine. Semin Cell Dev Biol. 2009; 20:646–655. [PubMed: 19508851]

Tang MH, Chen WC, Weir MD, Thein-Han W, Xu HHK. Human embryonic stem cell encapsulation in alginate microbeads in macroporous calcium phosphate cement for bone tissue engineering. Acta Biomater. 2012; 8:3436–3445. [PubMed: 22633970]

Unger RE, Dohle E, Kirkpatrick CJ. Improving vascularization of engineered bone through the generation of pro-angiogenic effects in co-culture systems. Adv Drug Deliv Rev. 2015; 94:116–125. [PubMed: 25817732]

Unger RE, Sartoris A, Peters K, et al. Tissue-like self-assembly in cocultures of endothelial cells and osteoblasts and the formation of microcapillary-like structures on three-dimensional porous biomaterials. Biomaterials. 2007; 28:3965–3976. [PubMed: 17582491]

Ventura M, Sun Y, Cremers S, et al. A theranostic agent to enhance osteogenic and magnetic resonance imaging properties of calcium phosphate cements. Biomaterials. 2014; 35:2227–2233. [PubMed: 24342727]

Villars F, Guillotin B, Amedee T, et al. Effect of HUVEC on human osteoprogenitor cell differentiation needs heterotypic gap junction communication. Am J Physiol Cell Physiol. 2002; 282:C775–785. [PubMed: 11880266]

Wang J, Wang L, Yang M, Zhu Y, Tomsia A, Mao C. Untangling the effects of peptide sequences and nanotopographies in a biomimetic niche for directed differentiation of iPSCs by assemblies of genetically engineered viral nanofibers. Nano Lett. 2014; 14:6850–6856. [PubMed: 25456151]

Wenger A, Stahl A, Weber H, et al. Modulation of in vitro angiogenesis in a three-dimensional spheroidal coculture model for bone tissue engineering. Tissue Eng. 2004; 10:1536–1547. [PubMed: 15588413]

Wernike E, Montjovent MO, Liu Y, et al. VEGF incorporated into calcium phosphate ceramics promotes vascularisation and bone formation in vivo. Eur Cell Mater. 2010; 19:30–40. [PubMed: 20178096]

Xu HHK, Thein-Han W. Prevascularization of a gas-foaming macroporous calcium phosphate cement scaffold via co-culture of human umbilical vein endothelial cells and osteoblasts. Tissue Eng Part A. 2013; 19:1675–1685. [PubMed: 23470207]

Zhang B, Yang S, Zhang Y, Sun Z, Xu W, Ye S. Co-culture of mesenchymal stem cells with umbilical vein endothelial cells under hypoxic condition. J Huazhong Univ Sci Technolog Med Sci. 2012; 32:173–180. [PubMed: 22528216]

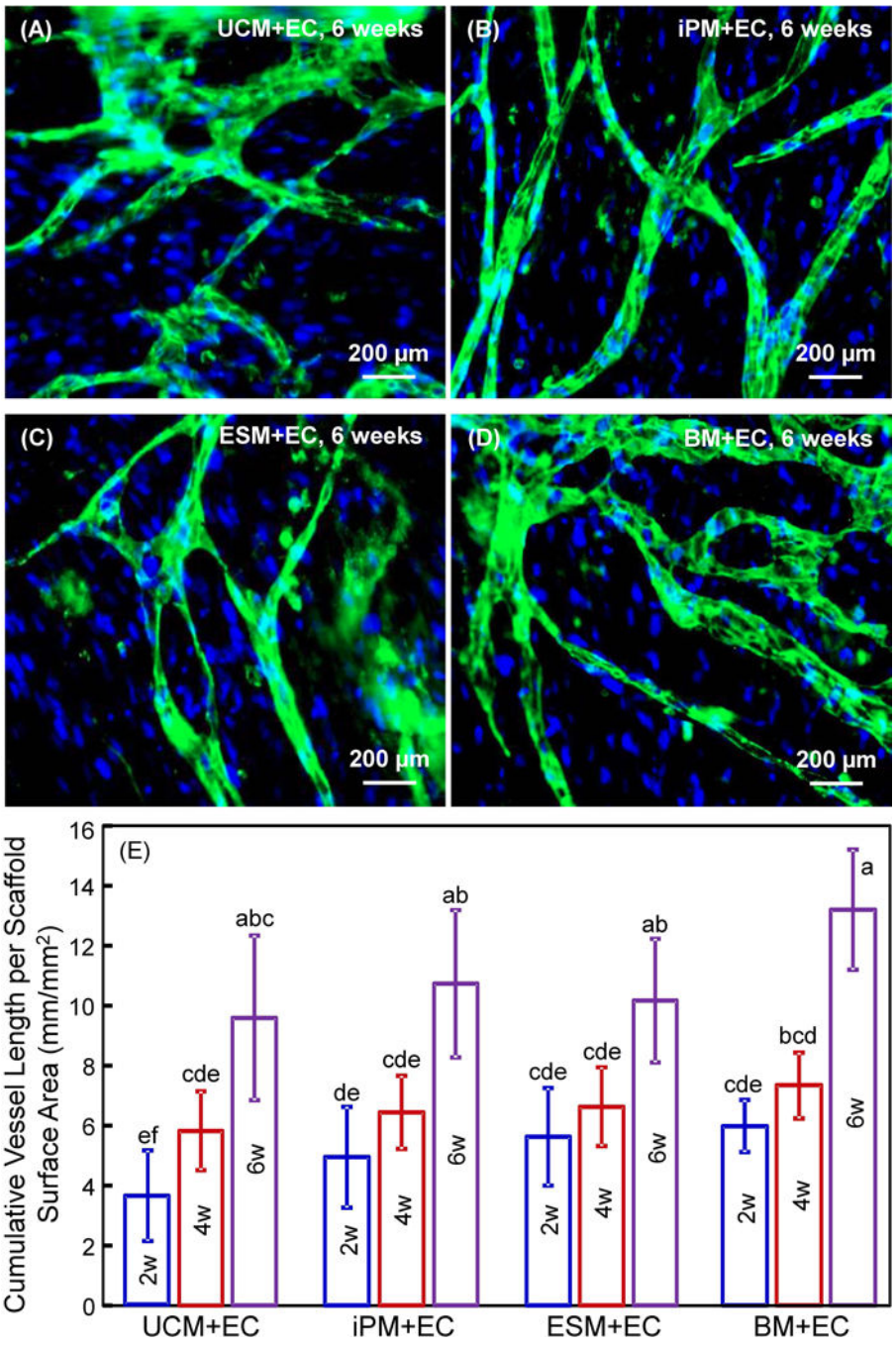

Figure 1.

hUVECs with hUCMSCs, hiPSC-MSCs, hESC-MSCs and hBMSCs had capillary-like structures. (A–D) Typical fluorescent images of coculture at 6 weeks with microcapillary structures on macroporous CPC-RGD. (E) Cumulative microcapillary length per scaffold surface area (mean ± sd; n = 5). hUCMSCs = UCM. hUVECs = EC. hiPSC-MSCs = iPM. hESC-MSCs = ESM. hBMSCs = BM. Week = w. Values that share the same letter (for example, the four groups at 6 weeks share the same letter a) are not significantly different

from each other ($p > 0.1$). Values indicated by different letters (without any letter that is the same) are significantly different from each other ($p < 0.05$).

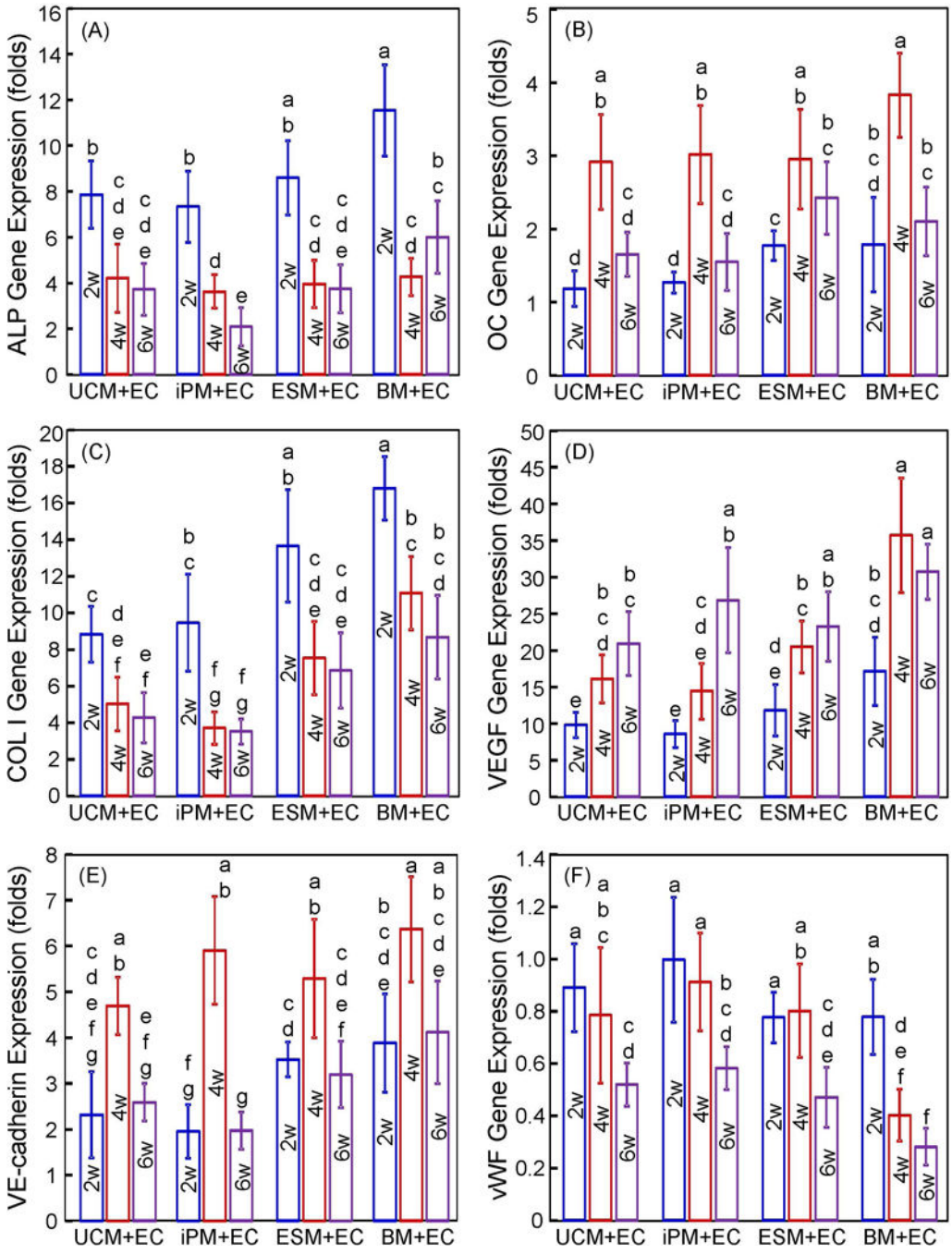

Figure 2.

Osteogenic and angiogenic gene expressions of cocultured hUVECs and MSCs: (A) ALP; (B) OC; (C) COL I; (D) VEGF; (E) VE-cadherin; and (F) vWF (mean ± SD; n = 5). hUCMSCs = UCM. hUVECs = EC. hiPSC-MSCs = iPM. hESC-MSCs = ESM. hBMSCs = BM. Week = w. In each plot, values that share the same letter are not significantly different from each other ($p > 0.1$). Values indicated by different letters (without any letter that is the same) are significantly different from each other ($p < 0.05$).

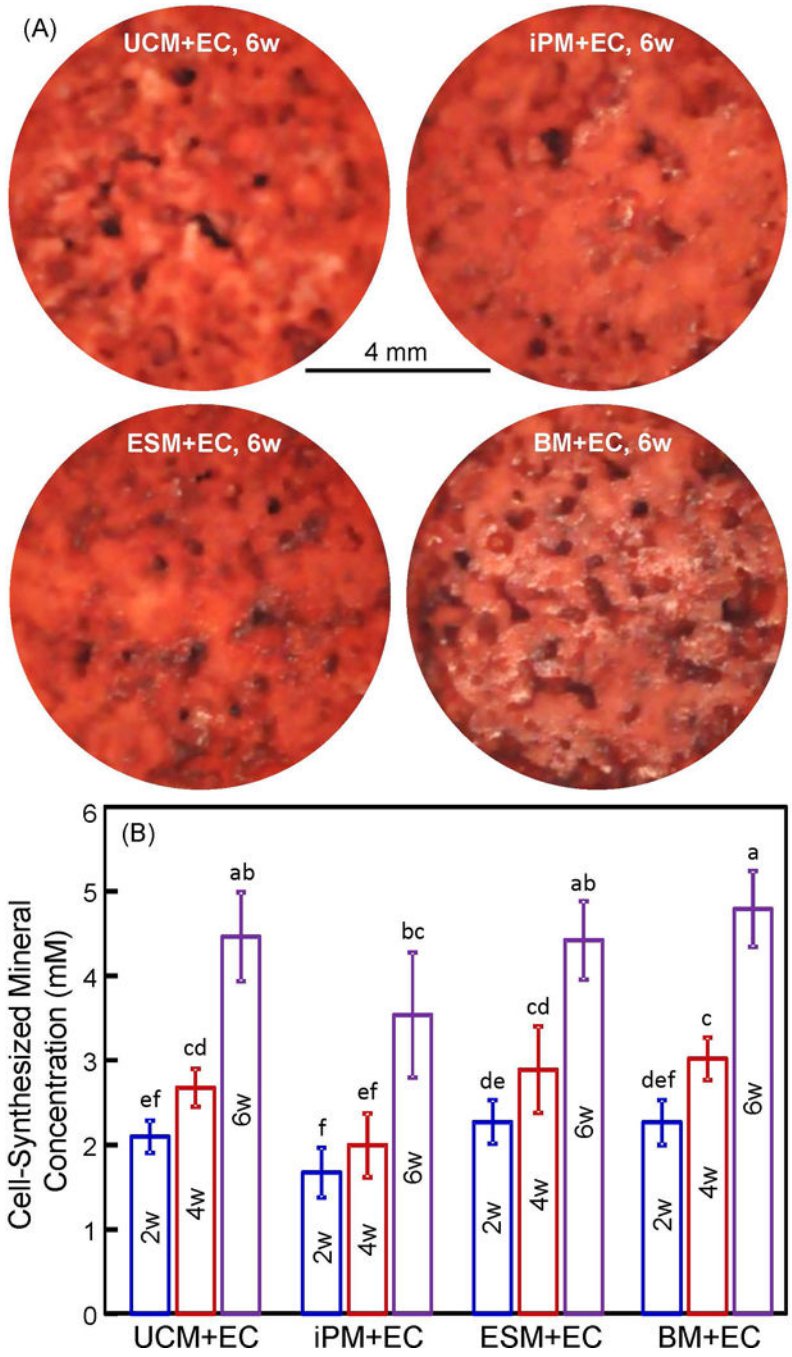

Figure 3.

Cocultured cell mineralization on macroporous CPC-RGD: (A) ARS of minerals by cells on CPC-RGD at 6 weeks, and (B) cell-synthesized mineral concentration (mean ± sd; n = 6). hUCMSCs = UCM. hUVECs = EC. hiPSC-MSCs = iPM. hESC-MSCs = ESM. hBMSCs = BM. Week = w. Values that share the same letter are not significantly different from each other ($p > 0.1$). Values indicated by different letters (without any letter that is the same) are significantly different from each other ($p < 0.05$).

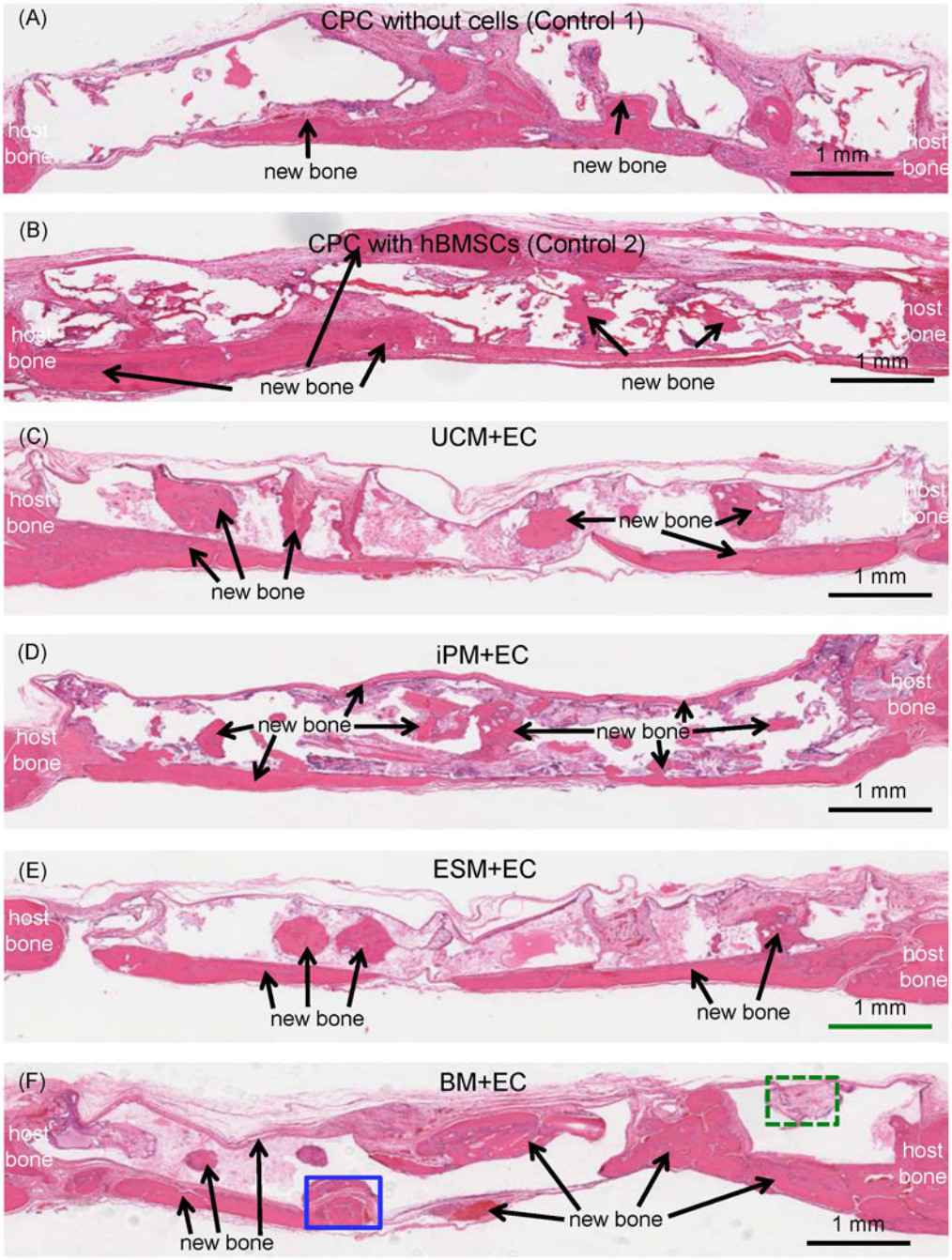

Figure 4.

Typical H&E staining histological images of critical-sized defects in rats at 12 weeks. The group name is listed in the middle of each image. The periosteal side of the defect is on the top, and the dura side is on the bottom, of the image. New bone (arrows) was observed in all groups. The blank areas in the images were CPC which became blank in H&E staining images due to decalcification.

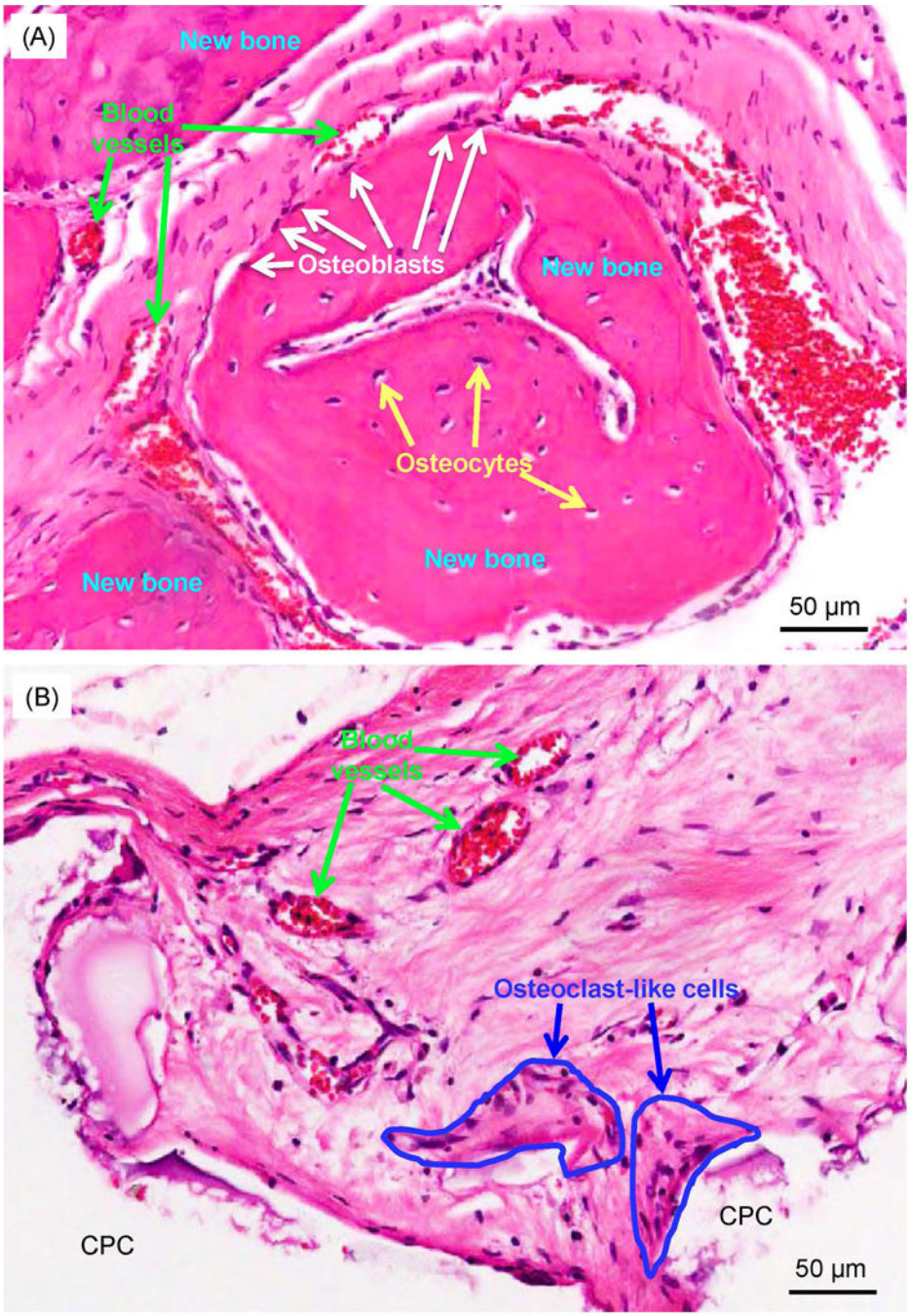

Figure 5.

High magnification images showing typical details in defects: (A) High magnification image of the solid-line rectangle in Fig. 4F, and (B) dotted-line rectangle in Fig. 4F. In (A), osteoblasts with a spindle morphology (white arrows) were found around new bone. Osteocytes (yellow arrows) were found inside new bone. New blood vessels (green arrows) were found around the new bone area. In (B), osteoclast-like multinuclear giant cells (encircled by blue lines) surrounded the CPC surface in the resorption lacunae. The CPC areas were blank in the H&E staining images due to decalcification.

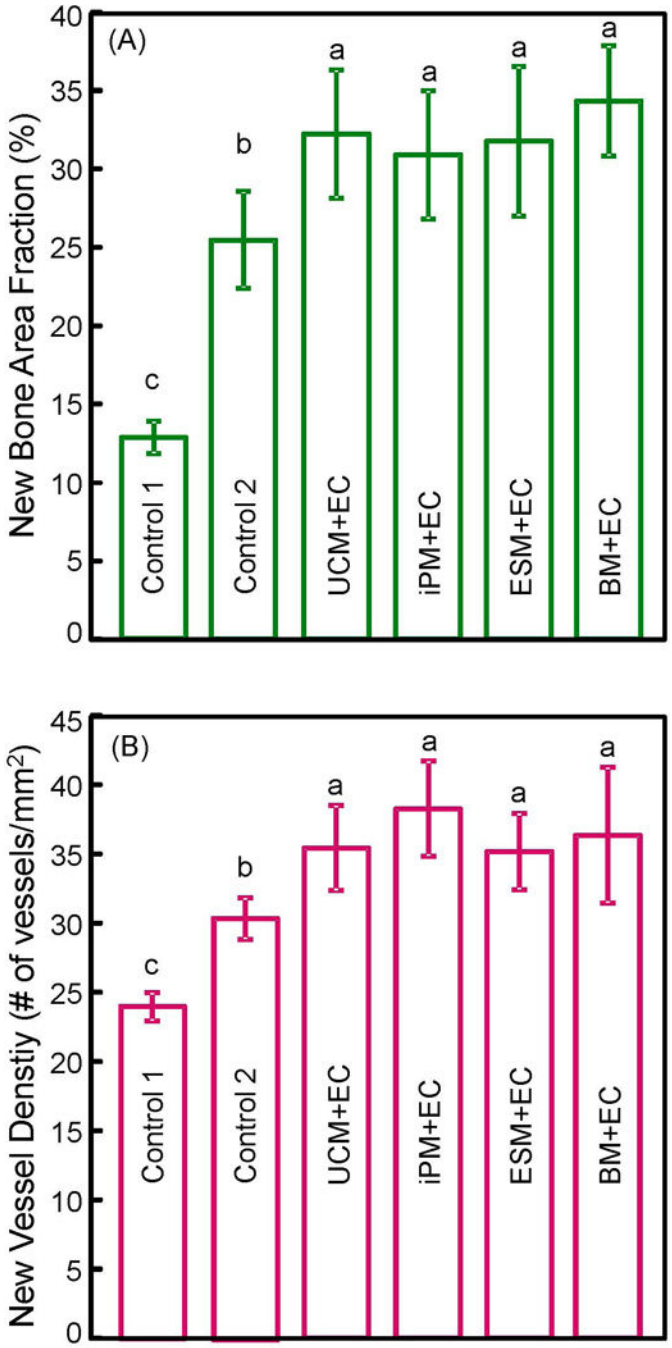

Figure 6.

Quantitative histomorphometry results for critical-sized cranial defects in rats at 12 weeks: (A) Percentage of new bone area, and (B) blood vessel density (mean ± sd; n = 5). Macroporous CPC-RGD containing cocultured cells showed greater new bone area and new blood vessel density than scaffold with hBMSCs alone (control 2) or without cells (control 1). Bars with dissimilar letters indicate significantly different values ($p < 0.05$).